Stem Cell Reports, Volume *8*

Supplemental Information

Resistance to Taxanes in Triple-Negative Breast Cancer Associates with the Dynamics of a CD49f+ Tumor-Initiating Population

Jorge Gómez-Miragaya, Marta Palafox, Laia Paré, Guillermo Yoldi, Irene Ferrer, Sergi Vila, Patricia Galván, Pasquale Pellegrini, Hector Pérez-Montoyo, Ana Igea, Purificación Muñoz, Manel Esteller, Angel R. Nebreda, Ander Urruticoechea, Idoia Morilla, Sonia Pernas, Fina Climent, María Teresa Soler-Monso, Ana Petit, Violeta Serra, Aleix Prat, and Eva González-Suárez

Supplementary Figure S1

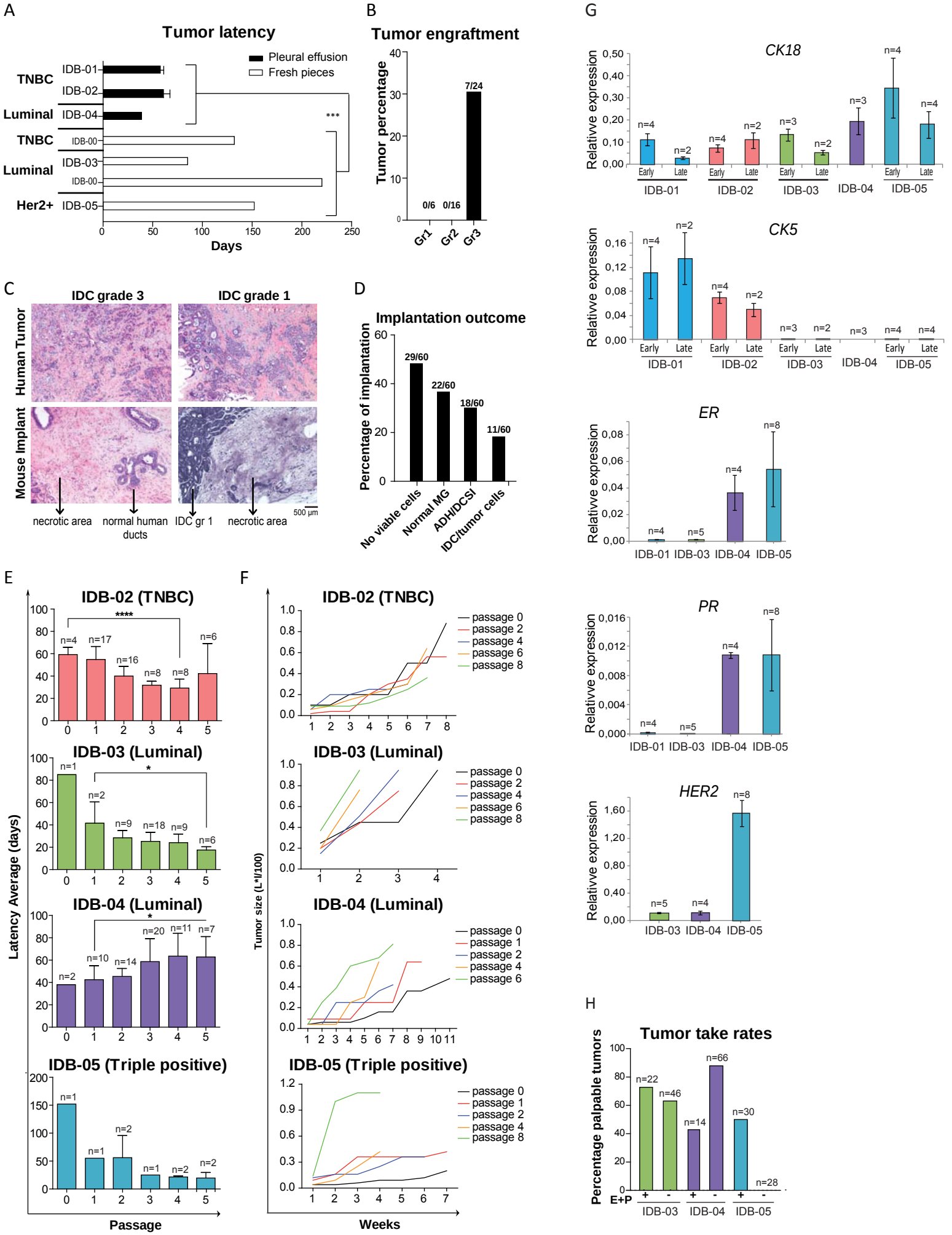

Supplemental Figure S2

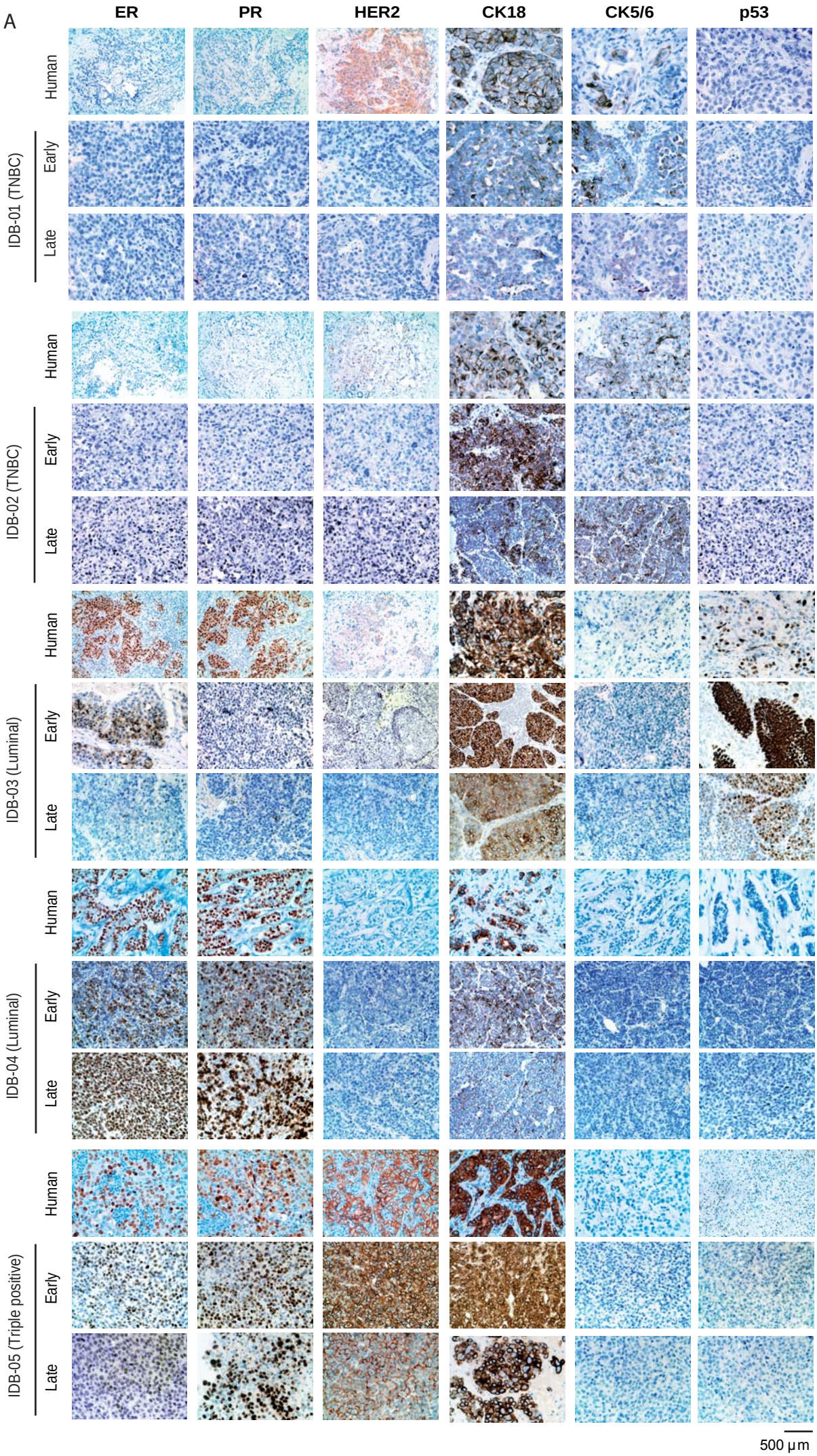

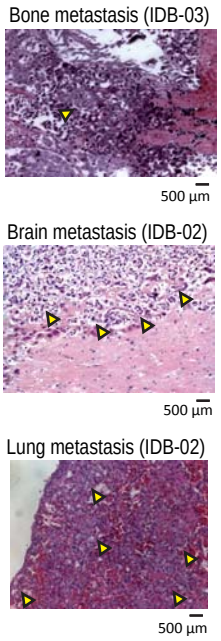

Supplemental Figure S3

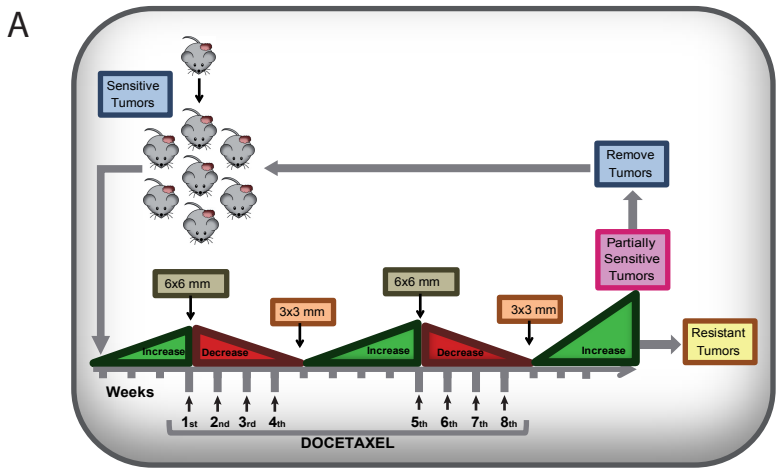

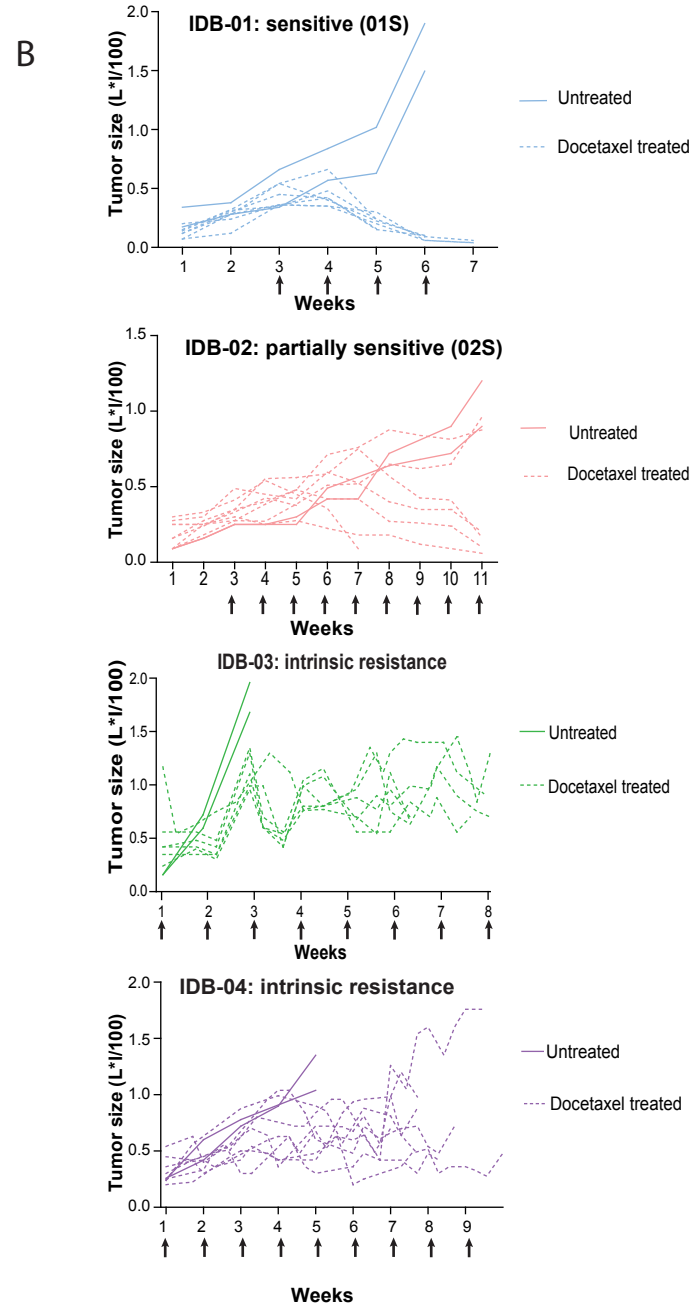

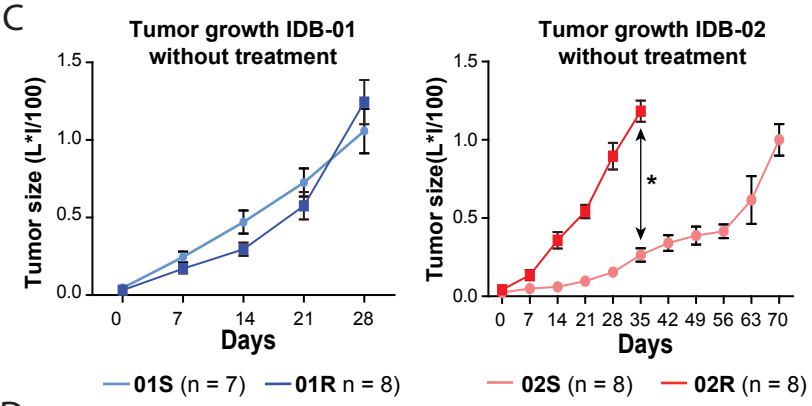

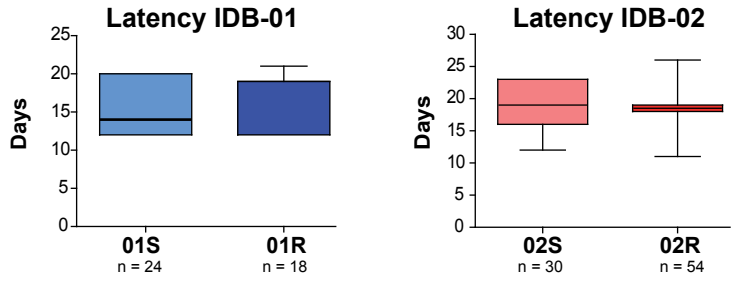

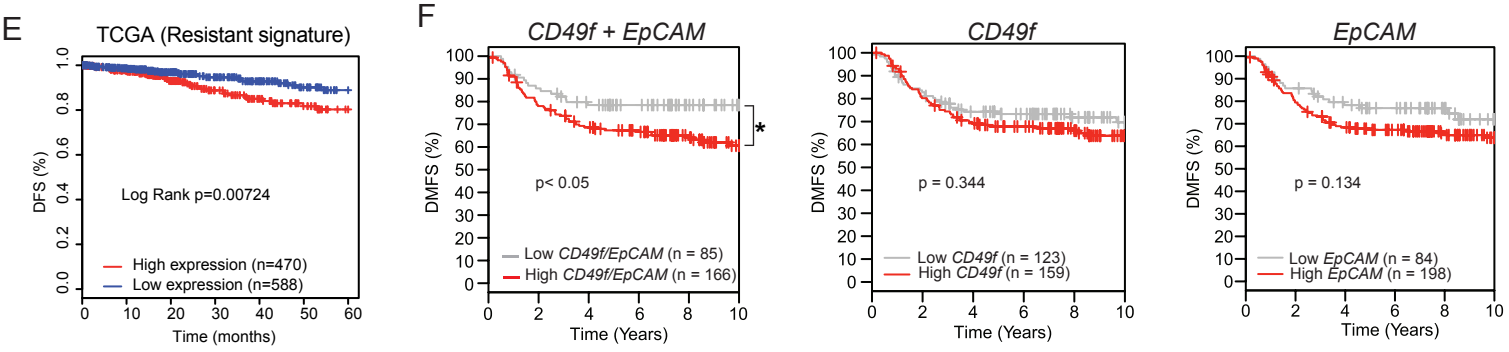

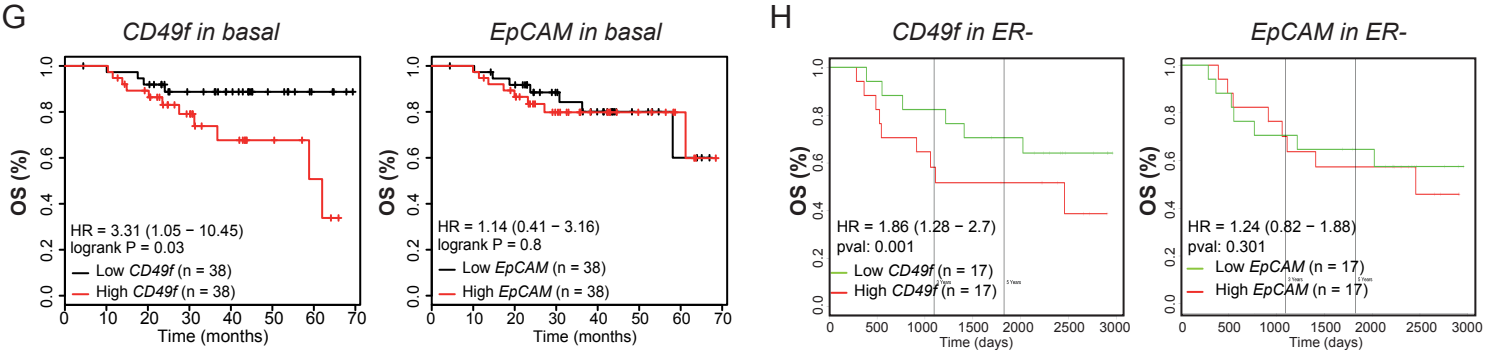

Supplemental Figure S4

A

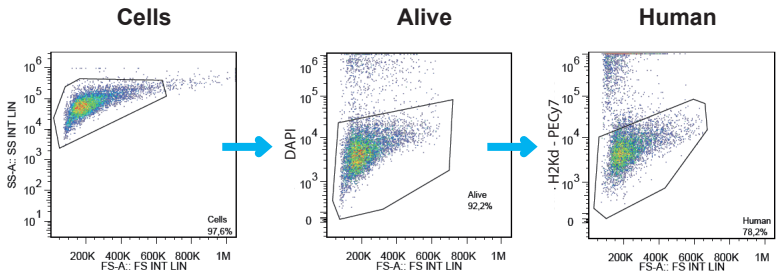

B

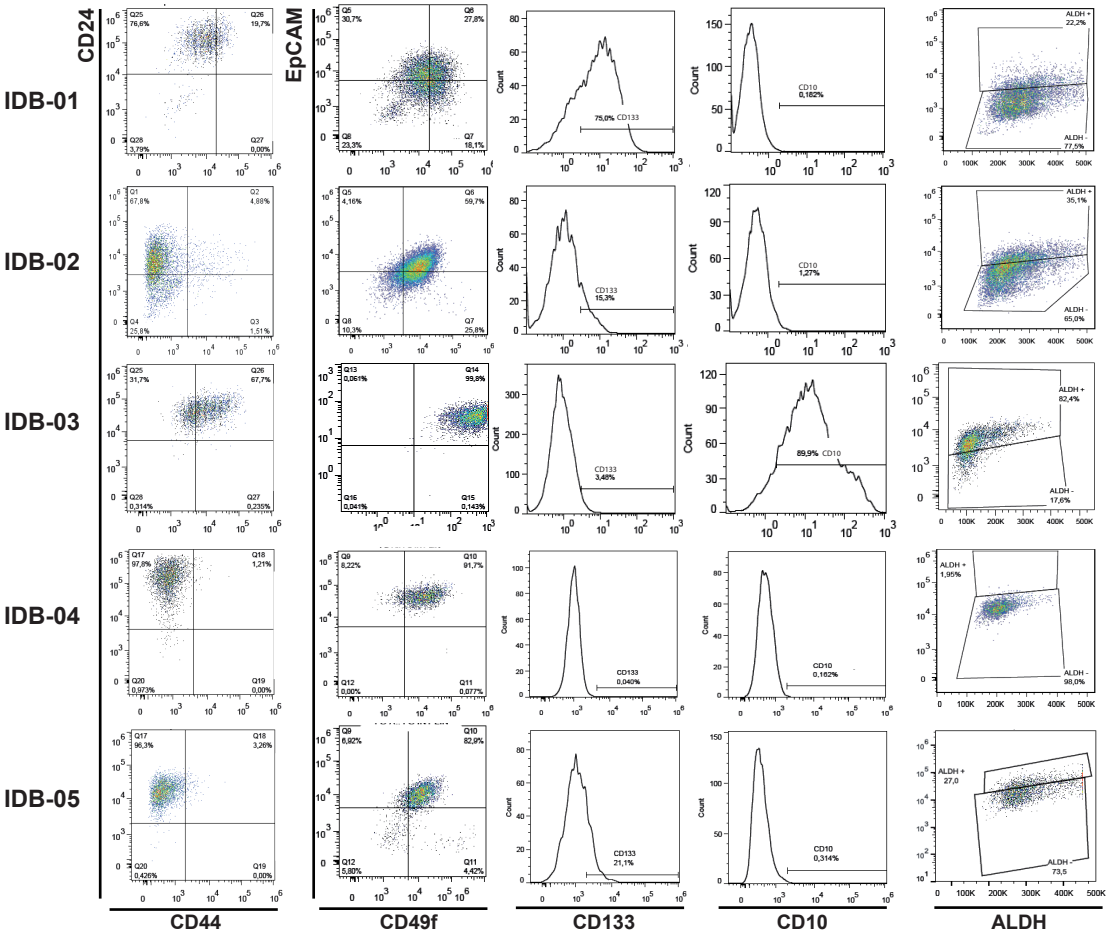

C

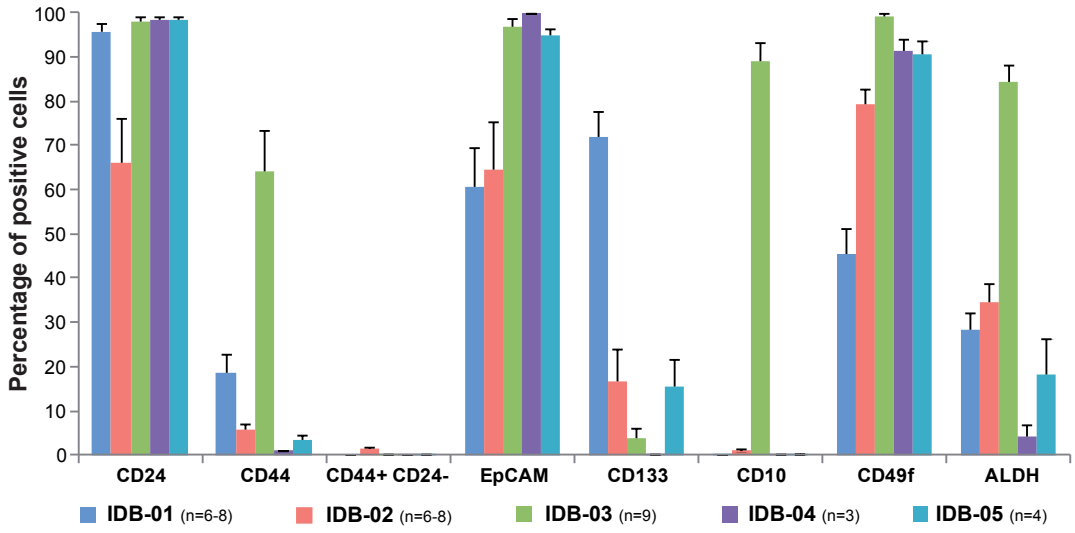

Supplementary Figure S5

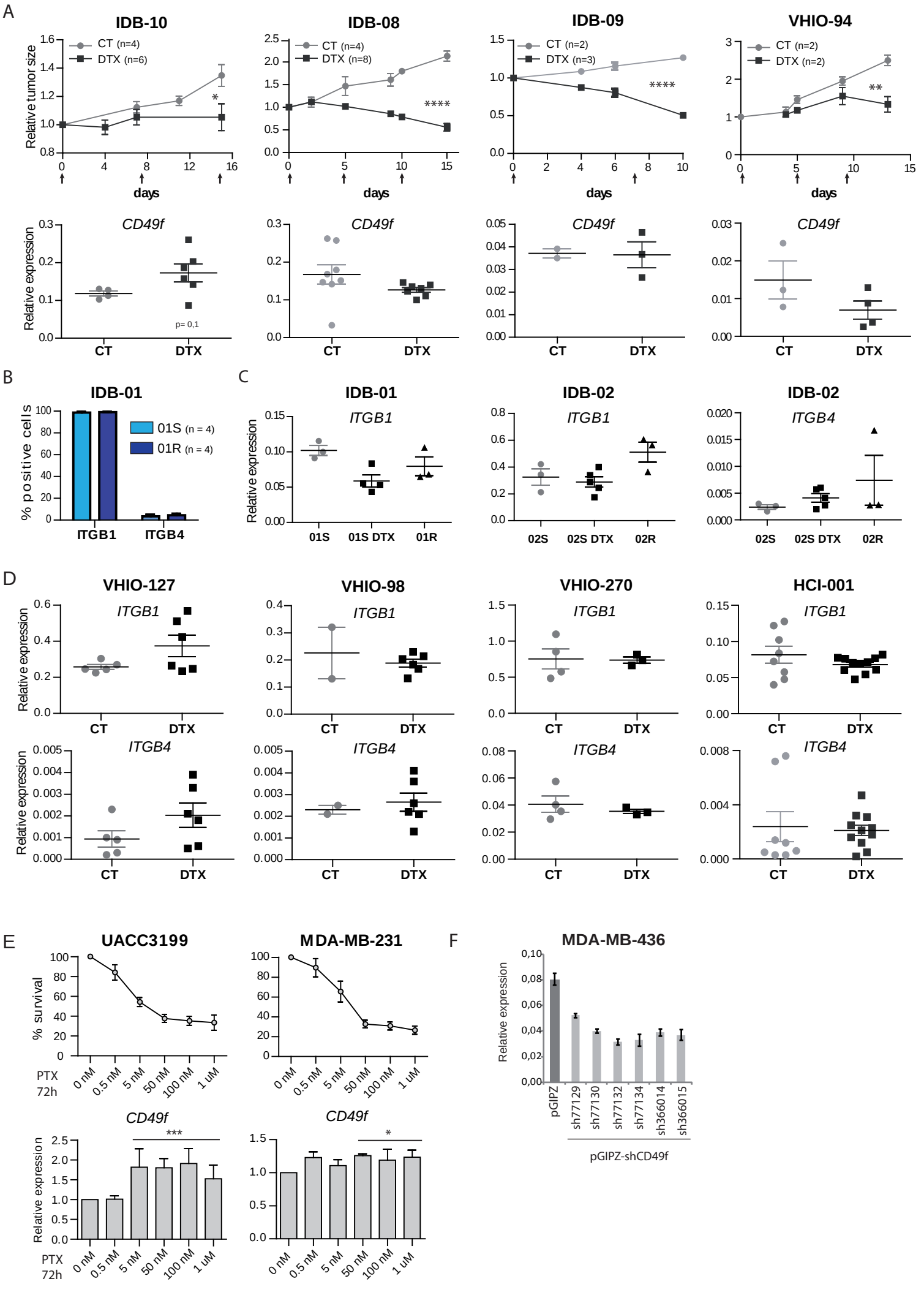

Supplemental Figure S6

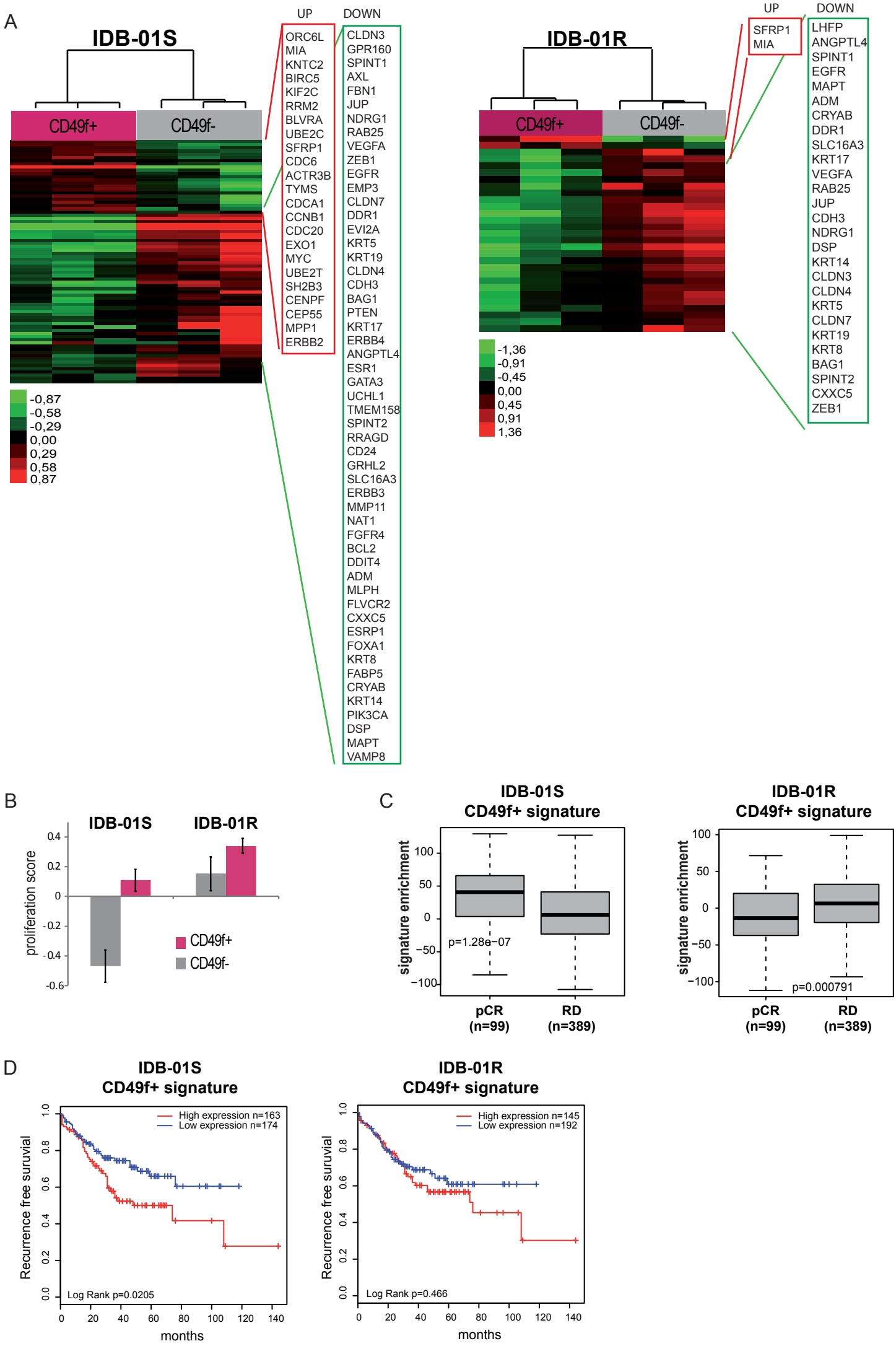

Supplemental Figure legends

Supplemental Figure S1. Generation of breast cancer PDX models (related to Figure 1 and Table 1)
A. Time in days until palpable lesions are detected in mice at first passage according to the source. All engrafted tumors were grade 3 and their subtype is shown. Mean values, SEM and p-values are shown (***, $0.001 < p < 0.0001$).
B. Percentage of palpable tumors engrafted relative to the total number of independent patient samples, depicted in pathological grade classification. Mice that did not survive for at least 60 days after surgery were excluded from the analyses. Total number of samples is indicated (n). Gr1 = grade 1; Gr2 = grade 2; Gr3 = grade 3.
C. Representative images of H&E staining of the original human tumors and the mouse mammary glands where they were implanted. No palpable lesions were detected in these mice and accordingly extensive necrotic areas were observed. However, viable human epithelial structures, mainly normal ducts, ADH (atypical ductal hyperplasia), DCIS (ductal carcinoma in situ) and occasionally IDC (invasive ductal carcinoma) or viable tumor cells were detected. Note that the morphology of IDC grade 1 is maintained in the mouse implant.
D. Percentage of mouse mammary glands showing human structures but not tumor growth. Quantification of indicated human structures in mouse mammary glands where no palpable lesions were detected is represented. MG = mammary glands. Only mice that survived for at least 60 days after tumor implantation were considered. Total number of MG analyzed is indicated (n).
E. Tumor latency (days) in each mouse tumor model at the indicated passages. Total number of tumors considered (n), mean, standard deviation and t-test p values for significant differences are shown (*, $0.01 < p < 0.05$; ****, $p < 0.0001$).
F. Tumor growth in mice, calculated as L x I (mm x mm)/100 versus time (weeks). Each line represents a representative tumor and each color represents a different passage as indicated. Week 1 is the time at which palpable tumors were first detected.
G. mRNA expression levels of indicated genes relative to *PPiA* at indicated passages: early (1^{st} to 5^{th}) and late (more than 10^{th}) measured by qRT-PCR. Total number of tumors analyzed is indicated (n). Determinations were done in triplicate and mean values were used for the calculations. Mean values for "n" independent tumors and standard deviations are shown.
H. Percentage of palpable tumors relative to the total number of tumors implanted with (+) or without (-) exogenous 17β-estradiol and progesterone pellets in luminal models. Total number of implanted mammary glands is indicated (n).

Supplemental Figure S2. Mouse PDX grafts resemble human tumors of origin at early passages but changes are observed at late passages in some models (related to Figure 1 and Table 1)
A. Representative images of estrogen receptor (ER), progesterone receptor (PR), HER2, cytokeratins (CK18, CK5/6) and p53 protein expression in human tumors of origin and tumors growing in mice of the indicated models at early (1^{st} to 2^{nd}) and later passages (4^{th} to 8^{th}) as determined by immunohistochemistry.
B. Representative H&E pictures of macroscopic metastasis.

Supplemental Figure S3. Docetaxel treatment in PDX models and association of CD49f and EpCAM expression with survival (related to Figure 2 and 3)
A. Schematic representation of docetaxel resistant tumors generation. Several tumors from each model were implanted in both mammary inguinal glands of 8 recipient NOD/Scid females. Tumor-bearing animals were individually identified and when tumors reached 6x6 of size, mice were treated with docetaxel (20 mg/kg i.p.) once a week as indicated. If the tumor volume decreases below 3x3 size treatment was interrupted and re-initiated when tumor volume increased again over the size of 6x6. After 10 to 12 doses, mice were sacrificed, tumors were excised and re-implanted in mice (second passage) to repeat the process until tumors become resistant.
B. Representative kinetics of tumor growth during docetaxel treatment in sensitive TNBC IDB-01S and IDB-02S tumors and resistant luminal tumors IDB-03 and IDB-04. Tumor size (v = Lxl/100) is shown over time (weeks). Each line represents one tumor and arrows indicate docetaxel treatments.
C. Tumor growth in the initially sensitive (IDB-01S and IDB-02S) and after resistance to taxanes was acquired (IDB-01R and IDB-02R). Total number of tumors analyzed (n), mean values and SEM are shown. (*, $0.01 < p < 0.05$).

D. Box and whiskers graph (min to max) showing time in days until palpable tumors are detected (tumor latency) in the initially sensitive (IDB-01S and IDB-02S) and after resistance to taxanes was acquired (IDB-01R and IDB-02R). Total number of tumors is shown (n).
E. Kaplan-Meier analyses of disease free survival (DFS) of the resistant signature identified in the TCGA database for breast tumors.
F. Kaplan-Meier analyses of distal metastasis free survival of basal-like tumors using *CD49f* and *EpCAM* mRNA expression independently and combined in the online GOBO database (Ringner et al., 2011).
G. Kaplan-Meier analyses of overall survival of basal-like tumors using *CD49f* and *EpCAM* mRNA expression in the clinical data set (GSE16446) from the TOP TRIAL (Desmedt et al., 2011) .
H. Kaplan-Meier analyses of overall survival of basal-like tumors using *CD49f* and *EpCAM* mRNA expression in the clinical data set (GSE42568) (Clarke et al., 2013) .

Supplemental Figure S4. Heterogeneous expression of CSC markers in PDX models and FACs gating (related to Figure 3)
A. Gating scheme. Analyzed cells were first gated as DAPI negatives (live cells) and H2Kd- (human cells).
B. Representative dot-plots and histograms of indicated markers in H2kD- human cells from each tumor model. The axes were established according to fluorescence minus one (FMO) controls or ALDH negative control.
C. Frequency of indicated markers within the human H2Kd- population analyzed by flow cytometry on established PDX. Total number of tumors analyzed (n), mean values and SEM are shown. Passage 7-14 was analyzed for all models

Supplemental Figure S5. No changes in ITGB1 and ITGB4 in docetaxel resistant tumors or residual disease (related to Figure 4 and 5)
A. Top panels: Tumor size of the indicated PDX tumors treated with docetaxel (20 mg/kg arrows) and corresponding controls relative to the size at the first day of treatment. Total number of tumors (n), mean, SEM and t-test p values are shown (*, $0.01 < p < 0.05$; **, $0.001 < p < 0.01$; ****, $p < 0.0001$). Bottom panels: *CD49f* mRNA expression levels relative to *PPiA* in tumors treated with docetaxel and untreated controls measured by qRT-PCR. Determinations were done in triplicates and means are used.
B. Frequency of ITGB1+ and ITGB4+ cells in H2Kd- human cells in IDB-01S and IDB-01R tumors measured by flow cytometry. Total number of tumors analyzed (n), mean values and SEM are shown.
C. *ITGB1* and *ITGB4* mRNA expression levels relative to *PPiA* in sensitive untreated tumors, residual disease after docetaxel treatment and tumors with acquired resistance in IDB-01 and IDB-02 models measured by qRT-PCR. No expression of *ITGB4* was found in IDB-01 tumors. Determinations were done in triplicates. Means and SEM are shown.
D. *ITGB1* and *ITGB4* mRNA expression levels relative to *PPiA* in tumors treated with docetaxel and in untreated controls of indicated PDX models measured by qRT-PCR. Determinations were done in triplicates.Means and SEM are shown.
E. Top panels. Percentage of surviving cells treated with indicated doses of paclitaxel for 72h. Bottom panels: *CD49f* mRNA expression levels in cells treated with paclitaxel relative to untreated controls. Mean values of 3 independent experiments, SEM and t-test p values for the higher concentrations are shown. (*, $0.01 < p < 0.05$; ***, $0.001 < p < 0.0001$)
F. Bars show *CD49f* mRNA expression levels relative to *PPiA* in the indicated TNBC cell lines stably infected with six independent shCD49f knock-down constructs and control vector (pGIPZ) measured by qRT-PCR. Determinations were done in triplicates and means are used.

Supplemental Figure S6. Molecular characterization of CD49f+ and CD49f- cell populations (related to Figure 6)
A. Supervised expression analysis of the genes found differentially expressed between CD49f+ and CD49f- cells within IDB-01S and -01R tumors. Each square represents the relative transcript abundance.
B. Expression of the PAM50 proliferation score across CD49f+ and CD49f- cells within IDB-01S and -01R tumors. Mean values and SEM are shown
C. Association of IDB-01S-CD49f+ or 01R-CD49f+ signatures with chemotherapy response in 508 patients with breast cancer (GSE25066). Response was measured as pathological complete response or residual disease. Total number of tumors analyzed (n), box and whiskers (min to max) graphs and mean values are shown.

D. Kaplan-Meier analysis of overall survival and distant metastasis free survival using sensitive and resistant CD49f+ signatures in the Perou extended database (Prat et al., 2010).

Supplemental Items

Supplemental Table S1. Characteristics of human tumors of origin and recipient mice (related to Table 1, Figure 1 and 2)

Source, histopathological status and clinical data available of the 61 human samples implanted; number, strain, survival of recipient mice and outcome after H&E examination of recipient mammary glands are shown. Samples excluded from the analysis are shown in red. Samples highlighted in yellow indicate established tumor models. IDC: invasive ductal carcinoma; ADH: atypical ductal hyperplasia; DCIS: ductal carcinoma in situ; QT: chemotherapy; HTP: hormonotherapy, n.d.: no data, n.e. not evaluable. MG: mammary gland.

Supplemental Table S2. Gene expression signatures and raw data (related to Figure 2, Figure 6 and S6)

Supplemental Experimental Procedures

Generation of PDX

A total of 61 samples from breast cancer patients, 54 from fresh primary tumor pieces obtained directly after surgery and 7 from cancer cells isolated from pleural effusions were transplanted into the fat pad of 90 immunodeficient mice. Three strains of immunodeficient mice have been used. Nude mice (Athymic Nude - Foxn1nu Harlan), NOD/ Scid (NOD.CB17-Prkdcscid/J; JAX via Charles River) and Scid/Beige (CB17.Cg-PrkdcscidLystbg-J/Crl, JAX via CR) mice (Carroll and Bosma, 1991). Mice were maintained in specific pathogen-free animal housing (IDIBELL). NOD/Scid and Scid/Beige mice were bred in our animal facility. Fresh primary human breast tumor fragments and cells isolated from pleural effusion were obtained from patients at the time of surgery or thoracocentesis, with informed written patient consent. Fragments of 30 to 60 mm^3 were implanted into cleared fat pad from 4^{th} mammary glands of 3-weeks-old NOD/Scid or Nude females and pellets of 17β-estrogen (0,1 mg) (Innovative Research of America) were implanted into the intraescapular fad pat; in the case of tumor cells isolated from pleural effusions, $3x10^6$ tumor cells were injected in 4th mammary glands of Nude, Scid/Beige or NOD/Scid females. Pathological characteristics of implanted samples, number and strain of host mice and engraftment outcome are shown in Supplementary Table S1. Orthotopic tumors appeared at the graft site 30 to 152 days after implantation and they were subsequently transplanted from mouse to mouse without clearing epithelia. In each passage, samples were collected, cryopreserved in DMSO-fetal bovine serum solution (1:10) as stock, or directly at -80ºC for gene expression analysis, and fixed with phosphate buffered saline (PBS) 10% formol, for histological studies.

Mice that died within 60 days after tumor implantation without developing tumor or samples without pathological data available were excluded from the analyses (15 samples, in red in Table S1). Tumor growth (engraftment) was analyzed in 46 patients´ samples implanted in 71 immunodeficient mice. In the first passage, palpable tumors from 7 patients were obtained; all of them derived from grade 3 tumors. We were able to successfully maintain 5 tumor lines by consecutive rounds of transplantation (yellow in table S1, indicated as IDB-01-IDB-05). To evaluate the influence of hormones ER+PR+ tumors were maintained in mice with or without 17β-estrogen (0,1 mg) progesterone (32,5 mg) pellets (Innovative Research of America) implanted into their intraescapular fad pat.

The additional models included (IDB-08-IDB-10) were generated following similar procedures, after implantation of fresh tumor pieces in the cleared fat pad of NSG (NOD.Cg-Prkdc^{scid} Il2rg^{tm1Wjl}/SzJ, JAX via Charles River) mice. All the *in house* generated PDX models were maintained by serial transplantation in the intact fat pad of Nod/Scid mice, except for IDB-08 which was maintained in NSG mice.

Model HCI001 (TNBC) was donated by A Welm and Y DeRose (DeRose et al., 2011) and was maintained in passage by serial transplantation over time in the fat pad of NSG mice. Models VHIO-93, -94, -98, -102, -127, -197, -270 and -288 (all of them TNBC, VHIO-127 is a BRCA1 mutant) were generated by subcutaneous implantation of primary tumor pieces (except for VHIO-127 and VHIO-288 which derived from metastasis) on the back of Nude mice as described previously (Bruna et al., 2016; Garcia-Garcia et al., 2012). The models from VHIO were collected and implanted in the intact fact pad of Nod/Scid mice in our animal facility to perform docetaxel treatments.

Tumor growth

Every mice was monitored for tumor incidence by palpation and visual inspection and for weight variations. Mice were sacrificed before tumors reached a diameter of 1,5 cm, or when 20% loss of their initial weight or deterioration of health was observed. Individual tumor size was calculated as L*l/100, with "L" being the largest diameter and "l" the smallest. Growth curves were established as a function of time. Tumor latency was recorded for all palpable tumors and mice. To emulate the clinical procedure tumors were surgically removed before they reached 1,5 cm of diameter and mice were left alive to determine the incidence of relapse and metastasis. We randomly sectioned the axillary mammary gland, lymph nodes and lungs of mice that survived longer than 60 days after primary tumor excision.

Histology and immunohistochemistry

Samples from patient or mouse tumors, and mammary fat pads of host mice that did not develope tumors were fixed in formalin immediately after resection and embedded into paraffin. Lungs, brain, liver, kidneys and other organs were collected following the same protocol. Bones were treated with 10% formic acid before were formalin fixation and paraffin embedding. For light microscopic examination 3-µm-thick sections were

stained with hematoxylin and eosin (H&E). Selected lungs from all models and brains from Model B were sectioned every 75-100 µm, stained with H&E and scored for metastasis. For immunohistochemical (IHC) studies 3-µm-thick sections were embedded in paraffin and incubated with antibodies against ER (1:30; DAKO, clon 1D5, IR657), PR (diluted; DAKO, clon 636, IR68), HER2 (1:350; DAKO, SK001), CK18 (diluted; DAKO, clon DC10, IR 618), CK5/6 (1:100; Zymed, clon D5/16B4, MAB1620) and p53 (1:50; Biogenex, AM195). Pre-treatment with citrate pH6 was done on slides stained for ER, PR, HER2, CK18 and p53 and with citrate pH9 on CK5/6 stained slides. Antibodies were detected using biotin-conjugated secondary antibodies (HRP; DAKO). The antigen-antibody complex was conjugated with streptavidin horseradish peroxidase and visualized with diaminobenzidine (Kit DAKO LSAB). Sections were counterstained with hematoxylin and appropriate positive and negative controls were used.

Breast cancer cells isolation

Fresh tissues were mechanically cut using the McIlwain tissue chopper and enzymatically digested with appropriate medium (Dulbecco's modified Eagle's medium [DMEM] F-12 (PAA), 0.3% Collagenase A (Roche Diagnostics, S.L.), 2.5U/mL Dispase (Gibco), 20 mM HEPES (Sigma-Aldrich), and antibiotics) 60 minutes at 37ºC with shacking. Samples were washed with Leibowitz-L15 medium (Gibco) supplemented with 10% fetal bovine serum (FBS) and penicillin/streptomycin between each step. Erythrocytes were eliminated by treating samples with hypotonic lysis buffer (ACK lysing buffer, Lonza Iberica) and incubated over night at 4ºC in the aforementioned Leibowitz-L15 medium. The following day, single epithelial cells were isolated by treating with trypsin (PAA Laboratories) 5 minutes at 37ºC and a mix of Dispase (Gibco life technologies, Invitrogen) DNAse (Invitrogen) for 10 minutes at 37ºC. Dead cells were first excluded by centrifugation with Lympholyte (Cedarlane laboratories) 800xg for 20 minutes and then 250xg for 10 minutes at room temperature. Cell aggregates were removed by filtering cell suspension with 40 µm filter and counted with Trypan Blue.

ALDH assay

Single cells were assessed for their ALDH activity using the ALDEFLUOR assay system (STEMCELL technologies). 4 x 10^5 cells were re-suspended in ALDEFLUOR buffer and activated ALDEFLUOR substrate was added. Immediately, half of them were separated in other tube with the inhibitor DEAB. The incubation was performed during 30 minutes at 37ºC. Mouse cells were excluded in flow cytometry using H2Kd-PECy7 (116622 from BioLegend). A population of 10,000 living cells was captured in all fluorescence-activated cell sorting (FACS) experiments. FACS analysis was performed using FACS Gallios cytometer (Beckman Coulter, Inc) and the FlowJo software package.

Therapeutic assays

For the generation of the docetaxel resistant-derived tumors, treatment started in mice bearing tumors of 6x6 mm size (L*l/100). Tumor growth and weight were evaluated twice a week. When tumor volume decreased below 3x3 mm, treatment was interrupted, and reinitiated when tumors re-grew over of 6x6 mm. Mice were ethically sacrificed after 10 to 12 doses of docetaxel when the tumor size surpassed a diameter of 1,5 cm or mouse weight decreased by 20%. Tumors were then excised, cut in pieces and re-implanted into new host mice (passage 2) in which docetaxel treatment was reinitiated following the same criteria, as shown in Supplementary Figure S3A.

For short term treatments, tumor bearing mice were treated with 2 to 5 doses of docetaxel, every 5-7 days for a period of 10 to 30 days, depending on tumors response. Mice were then sacrificed and tumors were analyzed for CD49f expression 3-5 days after the last dose of docetaxel, except for the most sensitive models that needed longer time to grow.

Lentiviral infection

Lentiviral infection was done following the manufacturer´s indications (Invitrogen). Briefly 293FT cells were used for the production of the virus. 293FT cells (5x106) were transfected with lentiviral pGIPZ empty or pGIPZ-shCD49f vectors (Dharmacon GE) and packaging (gag-pol, vsvg, rev) plasmids (Addgene) by calcium phosphate method. 25mM HEPES was added 16 h later. Virus supernatants were harvested 72h post transfection, centrigufated at 250G 5' and filtered with 0.22 µm filters. MDA-MB-436 cell lines were transduced in a ratio 1:3 with fresh growth medium and with 8µg/ml of polybrene. Plates were centrifuged 1 hour at 1.000 rpm at 37ºC to improve the infection. Selection started with puromycin antibiotic (Sigma-

Aldrich) at 1,5µg/ml. The resulting stable cell lines infected were maintained with 0,5 µg/ml . Medium was refreshed every three days. The following shCD49f sequences were tested: 77129: TATTCCATCTGCCTTGCTG; 77130:TAGTTACTGAATCTGAGAG; 77132: TTCTGAATATTAATCACAG; 77134: TTAGAAACAATACCTTTCC; 326014: ATTTCTAAAGCAATATCCT and 326015: TCAGTTGTACTTAAAACCA, and based on the results 77132 and 77134 were selected.

RNA extraction and RT-PCR

Total RNA from tissue was prepared with Tripure Isolation Reagent (Roche). Frozen tumor tissues were fractionated using the POLYTRON® system PT 1200 E (Kinematica). cDNA was produced by reverse transcription using 1 µg of RNA in a 35 µL reaction following manufacturer's instructions (Applied Biosystems). 20 ng/well of cDNA were used for the analysis performed in triplicate. Quantitative PCR was performed using the LightCycler® 480 SYBR green. Primer sequences are indicated below. Ct analysis was performed using LightCycler 480 software (Roche). All primers indicated below are in 5' → 3' direction.

hCD49f Forward	CTGGCCTCTTCATTTGGCTA
hCD49f Reverse	AAAATACTGTGGGGCTCCAAT
hEpCAM Forward	AATCGTCAATGCCAGTGTACTT
hEpCAM Reverse	TCTCATCGCAGTCAGGATCATAA
hPPiA Forward	ATGCTGGACCCAACACAAAT
hPPiA Reverse	TCTTTCACTTTGCCAAACACC
hCK18 Forward	TCAGCAGATTGAGGAGAGCA
hCK18 Reverse	GAGCTGCTCCATCTGTAGG
hCK5 Forward	ATCGCCACTTACCGCAAGCTGCTGGAG
hCK5 Reverse	AAACACTGCTTGTGACAACAGAG
hER Forward	ATCTCGGTTCCGCATGATGAATCTGC
hER Reverse	TGCTGGACAGAAATGTGTACACTCCAGA
hPR Forward	GGCATGGTCCTTGGAGGT
hPR Reverse	CACTGGCTGTGGGAGAGC
hHER2 Forward	TTCCTTCCTGCTTGAGTTCC
hHER2 Reverse	GRGCTGTTCCTCTTCCAACG
hITGB1 Forward	GCCGCGCGGAAAAGATG
hITGB1 Reverse	ACAATTTGGCCCTGCTTGTA
hITGB4 Forward	CCCCGAGGTAGGTCCAGG
hITGB4 Reverse	GTTTGCCAAGGTCCCAGAGA

Public clinical tools:

The web-based tools used include: Gene expression-based Outcome for Breast cancer Online (GOBO), comprising 1881 breast cancer-samples (Ringner et al., 2011) http://co.bmc.lu.se/gobo/gsa_information.pl, Kaplan Meier plotter (KM plotter), capable to assess the effect of 54,675 genes on survival using 5,143 breast cancer patients (Szasz et al., 2016) http://kmplot.com/analysis/, and PROGgeneV2, a tool that can be used to study prognostic implications of genes in various cancers, including breast (Goswami and Nakshatri, 2014) http://watson.compbio.iupui.edu/chirayu/proggene/database/index.php

Supplemental References

Bruna, A., Rueda, O. M., Greenwood, W., Batra, A. S., Callari, M., Batra, R. N., Pogrebniak, K., Sandoval, J., Cassidy, J. W., Tufegdzic-Vidakovic, A.*, et al.* (2016). A Biobank of Breast Cancer Explants with Preserved Intra-tumor Heterogeneity to Screen Anticancer Compounds. Cell *167*, 260-274 e222.

Carroll, A. M., and Bosma, M. J. (1991). T-lymphocyte development in scid mice is arrested shortly after the initiation of T-cell receptor delta gene recombination. Genes Dev *5*, 1357-1366.

Clarke, C., Madden, S. F., Doolan, P., Aherne, S. T., Joyce, H., O'Driscoll, L., Gallagher, W. M., Hennessy, B. T., Moriarty, M., Crown, J.*, et al.* (2013). Correlating transcriptional networks to breast cancer survival: a large-scale coexpression analysis. Carcinogenesis *34*, 2300-2308.

DeRose, Y. S., Wang, G., Lin, Y. C., Bernard, P. S., Buys, S. S., Ebbert, M. T., Factor, R., Matsen, C., Milash, B. A., Nelson, E.*, et al.* (2011). Tumor grafts derived from women with breast cancer authentically reflect tumor pathology, growth, metastasis and disease outcomes. Nat Med *17*, 1514-1520.

Desmedt, C., Di Leo, A., de Azambuja, E., Larsimont, D., Haibe-Kains, B., Selleslags, J., Delaloge, S., Duhem, C., Kains, J. P., Carly, B.*, et al.* (2011). Multifactorial approach to predicting resistance to anthracyclines. J Clin Oncol *29*, 1578-1586.

Garcia-Garcia, C., Ibrahim, Y. H., Serra, V., Calvo, M. T., Guzman, M., Grueso, J., Aura, C., Perez, J., Jessen, K., Liu, Y.*, et al.* (2012). Dual mTORC1/2 and HER2 blockade results in antitumor activity in preclinical models of breast cancer resistant to anti-HER2 therapy. Clin Cancer Res *18*, 2603-2612.

Goswami, C. P., and Nakshatri, H. (2014). PROGgeneV2: enhancements on the existing database. BMC Cancer *14*, 970.

Prat, A., Parker, J. S., Karginova, O., Fan, C., Livasy, C., Herschkowitz, J. I., He, X., and Perou, C. M. (2010). Phenotypic and molecular characterization of the claudin-low intrinsic subtype of breast cancer. Breast Cancer Res *12*, R68.

Ringner, M., Fredlund, E., Hakkinen, J., Borg, A., and Staaf, J. (2011). GOBO: gene expression-based outcome for breast cancer online. PLoS One *6*, e17911.

Szasz, A. M., Lanczky, A., Nagy, A., Forster, S., Hark, K., Green, J. E., Boussioutas, A., Busuttil, R., Szabo, A., and Gyorffy, B. (2016). Cross-validation of survival associated biomarkers in gastric cancer using transcriptomic data of 1,065 patients. Oncotarget *7*, 49322-49333.